Carcinogenesis vol.31 no.7 pp.1202–1210, 2010
doi:10.1093/carcin/bgq078
Advance Access publication April 15, 2010

HIF-2α-mediated activation of the epidermal growth factor receptor potentiates head and neck cancer cell migration in response to hypoxia

Xin Wang[1] and Abraham Schneider[1,2,*]

[1]Department of Oncology and Diagnostic Sciences, Dental School and [2]Marlene and Stuart Greenebaum Cancer Center, Program in Oncology, University of Maryland, Baltimore, MD 21201, USA

*To whom correspondence should be addressed. Tel: +410-706-7628; Fax: +410-706-6115;
Email: aschneider@umaryland.edu

Despite their individual key roles in promoting head and neck squamous cell carcinoma (HNSCC) progression and treatment resistance, little is known about the impact of intratumoral hypoxia on the activity of the epidermal growth factor receptor (EGFR) signaling pathway in this cancer type. Here, we show that in highly EGFR-expressing HNSCC cells, hypoxic stress triggers the activation of the EGFR and downstream targets, including Akt and phospholipase C (PLC) γ1. In support of these findings, we also demonstrate that EGFR activation takes place within hypoxic foci in a subset of human HNSCC tissues. Whereas hypoxia had no major effect on HNSCC cell proliferation, it markedly altered tumor cell shape by inducing morphological changes consistent with a more spindle-shaped, fibroblast-like morphology together with an enhanced migratory capacity. We found that hypoxia-induced EGFR activation and cell migration could be prevented by targeting EGFR signaling with the tyrosine kinase inhibitor tyrphostin, the phospholipase C inhibitor U73122, or by inhibiting the expression of the α subunit of hypoxia-inducible factor 2 via RNA interference or the topoisomerase II inhibitor etoposide. Our results position hypoxia-inducible factor-2α as a novel regulator of EGFR activation under low oxygen conditions, and suggest that hypoxia-induced EGFR signaling may promote a more aggressive phenotype in a fraction of HNSCC tumors. Because EGFR continues in the forefront as a highly attractive target in clinical oncology, further studies are warranted to define the mechanistic and therapeutic implications of the hypoxic response relative to the EGFR signaling pathway in head and neck cancer.

Introduction

Tumor microenvironmental pressures are major contributing factors in the progression of human cancer, including head and neck squamous cell carcinoma (HNSCC) (1–3). Nearly 45 000 new HNSCC cases are diagnosed each year in the USA, making this cancer type the sixth most common malignancy among Americans (4). About 30–40% of these patients will eventually die from their disease due, in part, to resistance to currently available therapeutic protocols (5). The identification of basic mechanisms by which microenvironmental cues impact HNSCC progression and therapeutic response is essential to design novel strategies to target a cancer type where locoregional invasion, lymph node metastasis and tumor recurrence are hallmarks of advanced disease (6).

Low oxygen levels are often found within growing HNSCC tumors (7,8). Indeed, tumor hypoxia has been strongly associated with head and neck cancer progression by compromising chemoradiation sensitivity and overall patient survival (9,10). The groundbreaking discovery of hypoxia-inducible factor-1α (HIF-1α) and HIF-2α as master driving forces of the cellular response to hypoxia has provided a fundamental molecular link to a long-standing clinical dilemma. As transcription factors, HIFs activate a vast array of genes encoding proteins commonly involved in angiogenesis, cell survival, migration and metastasis in a cell-type-dependent fashion (11). HIFs are heterodimers composed of two subunits, an oxygen-sensitive HIF-α and a constitutively active HIF-1β. Under normoxic conditions, HIF-α is subject to ubiquitination and proteasomal degradation via binding to the von Hippel-Lindau (VHL) tumor suppressor protein, a substrate recognition factor of an E3 ubiquitin-protein ligase (12). This phenomenon occurs when HIF-α is hydroxylated on specific proline residues by prolyl hydroxylases, which utilize O_2 and other cofactors as substrate. In addition, HIF-α hydroxylation by the asparaginyl hydroxylase factor inhibiting HIF-1 abrogates coactivator binding and transactivating activity (13,14). Under hypoxic conditions, hydroxylation, ubiquitination and proteolysis are inhibited resulting in HIF-α stabilization and translocation to the nucleus where in complex with HIF-1β promote gene transcription and expression (11).

Emerging evidence suggest that HIFs can drive oncogenesis by modulating the epidermal growth factor receptor (EGFR) signaling pathway through oxygen-dependent and -independent mechanisms (15–19). Because the EGFR has received much attention as a highly promising molecular target in different types of cancer, in particular head and neck cancer, it remains crucial to elucidate how tumor microenvironmental cues may affect EGFR function to ultimately improve therapeutic responses to targeted strategies (20). As the prototypical member of the ErbB family of receptor tyrosine kinases, the EGFR is overexpressed in 50–100% of HNSCC tumors (21). Increased EGFR gene copy number and high expression levels of EGFR ligands in HNSCC are considered strong predictors of tumor progression and poor clinical responses in a significant number of patients (22–24). Despite the negative role both the hypoxia and the EGFR pathways independently exert on HNSCC, their potential mechanistic interplay has remained elusive. Here, we show that in a subset of HNSCC cells and human-derived HNSCC tissues, where EGFR is highly overexpressed, hypoxic conditions led to EGFR pathway activation. Interestingly, exposure of HNSCC cells to hypoxic stress significantly increased cell migration and altered tumor cell shape as evidenced by a marked redistribution of the actin cytoskeleton and the formation of protrusive membrane structures. Inhibition of hypoxic HIF-2α expression or EGFR activity prevented these morphological changes and the development of the motile phenotype. Our results highlight an intimate link between tumor oxygenation and the EGFR pathway in HNSCC, and point to HIF-2α as a key promoter of EGFR-driven tumor cell migration in response to hypoxia.

Materials and methods

Cell culture, reagents and antibodies

The human-derived HNSCC cell lines HN4, HN6, HN12, HN13 and Hep-2 were kindly provided by Dr J. Silvio Gutkind (National Institute of Dental and Craniofacial Research, NIH, Bethesda, MD) and described previously (25). HNSCC cell lines were grown and maintained in Dulbecco's modified Eagle's medium (DMEM) supplemented with 10% fetal bovine serum, 100 units/ml penicillin, 100 μg/ml streptomycin and 250 ng/ml amphotericin B (Sigma, St Louis, MO) at 37°C in humidified air with 5% CO_2. Unless otherwise indicated, HNSCC cells were routinely grown to 60–70% confluence and serum starved for 24 h prior to any treatment. Hypoxic conditions were generated by placing cells in a humidified tightly sealed modular incubator chamber containing a triple gas mixture of 1% O_2, 5% CO_2 and 94% nitrogen as described previously (26). Normoxic HNSCC cells were cultured under atmospheric conditions (21% O_2) at 37°C in the presence of 5% CO_2. Recombinant human epidermal growth factor (EGF) was purchased from Axxora, LLC (San Diego, CA). The chemical inhibitors tyrphostin (EGFR tyrosine kinase inhibitor; Calbiochem, Gibbstown, NJ), U-73122 (phospholipase C [PLC] inhibitor;

Abbreviations: EGF, epidermal growth factor; EGFR, epidermal growth factor receptor; HIF, hypoxia-inducible factor; HNSCC, head and neck squamous cell carcinoma; PCR, polymerase chain reaction; siRNA, short interfering RNA; VHL, von Hippel-Lindau; PLC, phospholipase C; TGF-α, transforming growth factor-α.

Sigma), and etoposide (topoisomerase II inhibitor; Calbiochem) were all prepared as stock solutions and diluted in DMEM at the appropriate concentrations for tissue culture experiments. For western blotting, the following primary antibodies were used from Cell Signaling Technology (Danvers, MA): rabbit monoclonal against phospho-EGFR (Tyr1173; 1:1000), phospho-ERK1/2 (Thr202/Tyr204; 1:1000), total S6 (1:1000), HIF-1α (1:500), and rabbit polyclonal against phospho-Akt (Ser473; 1:1000), total Akt (1:1000), total ERK1/2 (1:1000), phospho-S6 (1:1000), phospho-PLC-γ1 (1:500) and PLC-γ1; 1:1000). Rabbit polyclonal against HIF-2α (1:250) was obtained from Novus Biologicals (Littleton, CO). Rabbit polyclonal against total EGFR (1:2000) and mouse monoclonal against α-tubulin (1:1000) were purchased from Santa Cruz Biotechnology (Santa Cruz, CA). Secondary horseradish peroxidase-linked sheep antimouse or donkey antirabbit immunoglobulin G antibodies were obtained from Amersham Biosciences (Piscataway, NJ). For immunofluorescence stainings, we utilized primary mouse monoclonal antibody against β-actin (Sigma; 1:200) and rabbit polyclonal antibody against vinculin (1:100; Santa Cruz). As secondary antibodies, tetramethylrhodamine isocyanate-labeled goat antimouse immunoglobulin G (1:500; Invitrogen, Carlsbad, CA) or fluorescein isothiocyanate-labeled goat antirabbit immunoglobulin G (1:500; Sigma) were used. For immunohistochemistry, we used primary rabbit polyclonal antibodies against Glut-1 (1:500; Millipore, Billerica, MA), total EGFR (1:100; Santa Cruz) and phospho-EGFR (Tyr 992) (1:100; Cell Signaling). Mouse monoclonal antibody ep190b against HIF-2α (1:200) was obtained from Novus Biologicals. Biotinylated secondary antibodies were purchased from Vector Laboratories (Burlingame, CA).

RNA interference

Short interfering RNA (siRNA)-based experiments were performed as previously published (26). Briefly, HNSCC cells were plated at 10 000–15 000 cells per cm^2 overnight in complete DMEM. The following day, transfections were performed following the dilution of commercially available siRNA duplexes targeting HIF-1α or HIF-2α with Hiperfect transfection reagent and serum-free, antibiotic-free DMEM according to manufacturer's recommendations (Qiagen, Valencia, CA). Cells transfected with a non-targeted control siRNA (Qiagen) were included in all experiments. The next day following transfections, cells were serum starved and then exposed to either normoxia or hypoxia for the indicated times.

MTS assay

The effect of hypoxia on HNSCC cell proliferation was evaluated through a colorimetric assay by using the CellTiter 96® AQueous One Solution (MTS) reagent following the manufacturer's protocol (Promega, Madison, WI). HNSCC cells were plated overnight in triplicate in 96-well plates at a density of 5000–10 000 cells per cm^2. The following day, cells were either exposed to hypoxia or normoxia. After 72 h, MTS reagent was added directly to each culture well, incubated at 37°C for 1–2 h and absorbance at 490 nm was measured in a microplate reader.

Wound closure motility assay

Cells were grown to near confluency onto six-well plates in complete DMEM. Several uniform streaks (∼25–30 μm in width) were made on the cell monolayer with a p10 micropipette tip as previously described (27). Before placing cells under normoxia or hypoxia, cells were washed twice in phosphate-buffered saline (PBS) to remove cell debris and the medium was replaced with serum-free DMEM supplemented with 5 μg/ml mitomycin (Sigma) to inhibit cell proliferation. Migrating cells toward the acellular area of the wells were photographed at 0 and 8 h of incubation under normoxia or hypoxia with a digital camera attached to an inverted Nikon phase contrast microscope. To determine the width of the remaining wound relative to treatment conditions, the Image J 1.41o software program (National Institutes of Health, Bethesda, MD) was used to measure 10 randomly selected regions between wound margins per scratch. For each condition, the average width of the remaining wound was calculated and plotted.

In vitro *migration assay*

HNSCC cell migration assay was measured based on the Boyden chamber principle by using the QCM chemotaxis 24-well cell migration colorimetric assay (Millipore) in accordance with the manufacturer's instructions. Briefly, following 24-h serum starvation, a 24-well dish was used to plate HNSCC cells onto an insert containing an 8-μm pore size polycarbonate membrane (top compartment). The bottom compartment of the well was filled with serum-free DMEM. Following a 5-h exposure to normoxia or hypoxia, the polycarbonate membrane was removed and the cells that have migrated through were stained with the recommended staining solution. The dye was subsequently extracted, transferred to a 96-well plate and detected on a microplate reader at 560 nm. When chemical inhibitors were used, they were added to the medium in the bottom compartment 30 min prior to exposure to hypoxia.

Western blotting

After isolation of whole cell lysates, equal amounts of protein were separated by sodium dodecyl sulfate–polyacrylamide gel electrophoresis, electrophoretically transferred onto polyvinylidene difluoride membranes and immunodetection was performed as previously described (26).

RNA isolation, complementary DNA synthesis and polymerase chain reaction amplification

Total RNA was extracted from cells using Trizol reagent (Invitrogen). Total RNA (2 μg) was reverse transcribed to complementary DNA using the SuperScript II kit (Invitrogen) with oligo dT according to the manufacturer's instructions. Polymerase chain reaction (PCR) amplification was performed by using PCR Master Mix (Promega) together with 2 μl complementary DNA and specific primers. The following primers were obtained from Invitrogen: HIF-2α (forward 5′- GTCTCTCCACCCCATGTCTC-3′; reverse 5′-GGTTCTTC-ATCCGTTTCCAC-3′); transforming growth factor-α (TGF-α) (forward 5′-TCGCTCTGGGTATTGTGTG-3′; reverse 5′-GACCTGGCAGCAGTGTAT-CA-3′); EGFR (forward 5′-CTCAGCCTCCAGAGGATGTTC-3′; reverse 5′-CAGGGTTGTTGC TGAACCGCA-3′); β-actin (forward 5′-CGTACCACT-GGCATCGTGAT-3′; reverse 5′-GTGTTGGCGTACAGGTCTTTG-3′). PCR was performed in a thermocycler with the following cycling parameters for 25 cycles: 94°C for 30 s, 55°C for 30 s, and 72°C for 45 s. PCR products were size-fragmented on a 1.5% agarose/Tris–acetate–ethylenediaminetetraacetic acid gel.

Enzyme-linked immunosorbent assay.

To measure the concentration of different EGFR ligands in conditioned medium (100 μl sample volume), an array-based multiplex sandwich enzyme-linked immunosorbent assay was performed by RayBiotech (Norcross, GA).

Immunohistochemistry

Human HNSCC tissue sections were obtained from the University of Maryland Pathology Biorepository and Research Core in accordance with the University of Maryland, Baltimore Institutional Review Board standards and guidelines involving the use of anonymous tissues. Tissue slides were dewaxed in xylene, hydrated through graded alcohols and distilled water, and washed thoroughly in PBS. For immunostaining against Glut-1, EGFR or phospho-EGFR antigen retrieval was performed in a microwave (20 min) by using 10 mM citrate buffer (pH 6). Following incubation with 3% hydrogen peroxide in PBS (30 min), slides were washed in PBS and incubated in blocking solution (2.5% normal horse serum) for 1 h at room temperature. Sections were then incubated with the primary antibodies diluted in blocking solution overnight at 4°C. After washing with PBS, slides were incubated with biotinylated secondary antibodies (1 h; 1:400), followed by the avidin biotin complex method (Vector R.T.U. Stain Elite, avidin biotin complex kit; Vector Laboratories) for 30 min. Slides were washed and developed in 3,3-diaminobenzidine under microscope control and counterstaining with Harris hematoxylin. For HIF-2α immunostaining, antigen retrieval was performed with Tris–ethylenediaminetetraacetic acid buffer (10 mM Tris base, 1 mM ethylenediaminetetraacetic acid and 0.05% Tween 20; pH 9) in a microwave for 20 min. Then, the Catalized Signal Amplification II biotin-free tyramide signal amplification system from Dako-Cytomation (Carpinteria, CA) was used following the manufacturer's instructions. Images were taken with a SPOT digital camera attached to an Axiophot microscope (Zeiss, Thornwood, NY).

Immunofluorescence

Cells were grown to subconfluency on sterile glass cover slips in six-well plates, and exposed to either normoxia or hypoxia for 6 h. Cells were then washed with PBS containing 5 mM/l ethyleneglycol-bis(aminoethylether)-tetraacetic acid, fixed with 4% formaldehyde PBS for 20 min, permeabilized with 0.5% Triton X-100 PBS for 15 min, and blocked with 3% bovine serum albumin PBS for 1 h at room temperature. Cells were incubated with 100 μg/ml rhodamine-conjugated phalloidin (Sigma) at room temperature for 20 min. Alternatively, following blocking with 3% bovine serum albumin PBS for 2 h at 4°C, cells were incubated overnight at 4°C with primary antibodies against actin and vinculin, then washed thrice in PBS containing 5 mM/l ethyleneglycol-bis(aminoethylether)-tetraacetic acid and incubated 1 h at room temperature with fluorescein isothiocyanate-labeled or tetramethylrhodamine isocyanate-labeled secondary antibodies. Following either of these immunostaining procedures, coverslips were washed thrice in PBS, mounted on glass slides, and images were captured and analyzed with a Nikon Ellipse TE 2000-S confocal microscope and Laser Sharp 2000 (5.2) software (Bio-Rad, Hercules, CA).

Statistics

Student's *t*-test for independent analysis or analysis of variance followed by Bonferroni's multiple comparison tests were applied to analyze differences between experimental groups. Data were analyzed and presented by using

the GraphPad (La Jolla, CA) software program. $P < 0.05$ were considered statistically significant. Data are presented as mean ± SEM. All assays were repeated at least twice with similar results.

Results

Hypoxia induces EGFR activation in HNSCC cells

Despite their widely accepted role in oncogenesis, it is still unclear whether hypoxic stress contributes to EGFR pathway activation in HNSCC. Recent information reporting hypoxic control of the EGFR mitogenic pathway in other cellular systems prompted us to begin exploring potential regulatory mechanisms linking hypoxia to the EGFR pathway in HNSCC. Human-derived HNSCC cell lines with variable levels of EGFR expression were exposed to hypoxia under serum-repleted conditions for 24 h and the active EGFR status was evaluated by immunoblotting as judged by the phosphorylation of tyrosine 1173. Within this panel of cells, we found that only HN6 and HN13 cells had a variable basal, constitutive activation of the receptor that was increased by hypoxia (28) (Figure 1A). Differences in EGFR phosphorylation levels between normoxic versus hypoxic HN6 and HN13 cells became more evident when cells were cultured under serum-deprived conditions (Figure 1B). These results suggested that EGFR expression levels in a subset of HNSCC cells may be a critical determinant for relaying oncogenic signals in response to reduced oxygenation. In fact, we found that EGFR activation in these highly EGFR-expressing cells occurred within 2 h following hypoxia, whereas no EGFR phosphorylation was detected in HN4 cells at any time point (Figure 1C).

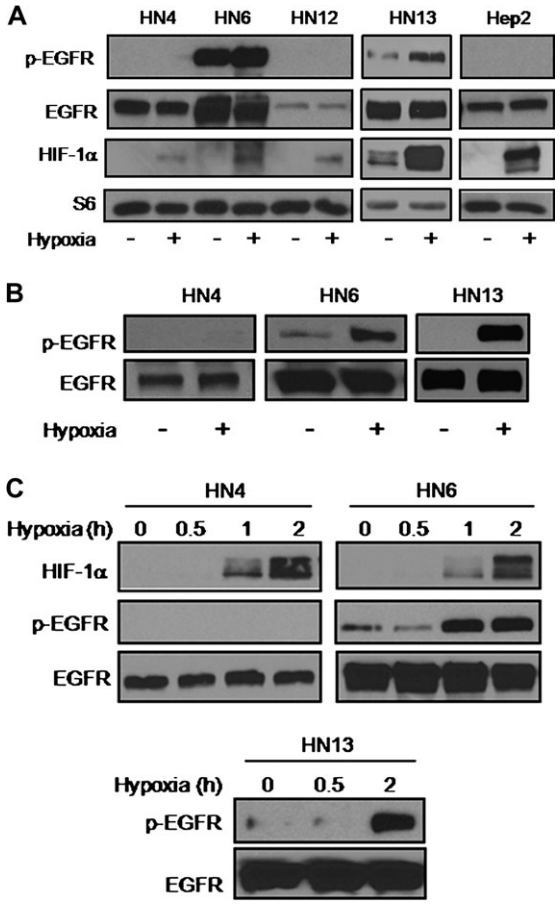

Fig. 1. Hypoxia activates EGFR in highly EGFR-overexpressing HNSCC cells. (**A**) Serum-repleted HNSCC cell lines were exposed for 24 h to normoxia or hypoxia. Western blots evaluating the phosphorylation status of EGFR. Increased HIF-1α expression validated hypoxic response in all cell lines. Total S6 is shown as loading control. (**B**) Western blots obtained from whole cell lysates isolated from serum-starved, hypoxic HN6 and HN13 cells show a marked increase in phosphorylated EGFR (pEGFR) expression compared with their normoxic counterparts or HN4 cells treated under similar conditions. (**C**) Time-dependent hypoxic activation of EGFR was triggered only in highly EGFR-overexpressing HN6 and HN13 cells.

HIF-2α mediates EGFR pathway activation in HNSCC cells

To gain insight into the signaling mechanisms linking hypoxia to EGFR activation, HN6 cell lysates were isolated at different time points following hypoxia to determine HIF-α levels and the phosphorylated status of EGFR and several downstream effectors belonging to the phosphoinositide-3-kinase/Akt, mitogen-activated protein kinase, mammalian target of rapamycin and PLC-γ1/protein kinase C pathways (29). As seen in Figure 2A, HIF-1α and HIF-2α levels appear to accumulate differentially following hypoxia. Whereas HIF-1α was detected within 2 h, HIF-2α levels started to rise as early as 15–30 min. A sharp declined in phosphorylated EGFR, Akt and PLC-γ1 expression was seen within 15 min following hypoxic stress (Figure 2A); however, within 1 h, the phosphorylated status of these proteins returned to basal levels and increased steadily for at least 6 h. These events appeared to parallel the time-dependent accumulation of HIF-2α but not HIF-1α. Conversely, ERK1/2 was rapidly induced within 15 min and returned to basal levels thereafter, suggesting an inverse expression pattern when compared withHIF-2α, phospho-EGFR, phospho-Akt and phospho-PLC-γ1 levels. Meanwhile, the phosphorylated status of ribosomal S6, a well-known surrogate marker of mammalian target of rapamycin pathway activation remained elevated and unaffected by hypoxia, supporting previous findings by our group (26). Because of the time-dependent correlation of HIF-2α with the activation of the EGFR pathway, we next utilized RNA interference to define the roles played by HIFs in promoting EGFR activity. Our findings revealed that EGFR phosphorylation was markedly decreased in HIF-2α siRNA-transfected HN6 and HN13 cells. In contrast, phospho-EGFR levels were either slightly decreased or unchanged when HIF-1α was knocked down in these cells (Figure 2B). Suppression of EGFR activation in hypoxic HIF-2α siRNA-transfected HN6 cells also prevented Akt and PLC-γ1 phosphorylation, confirming the dependency of these signaling proteins on hypoxia-induced EGFR activity (Figure 2C). Interestingly, we found that TGF-α, a well-known EGFR ligand and HIF-2α target gene (15), was the only EGFR ligand significantly increased in conditioned medium obtained from control siRNA-transfected HN6 cells exposed to hypoxia for 2 h. As expected, TGF-α levels were dramatically reduced in hypoxic HIF-2α siRNA-transfected cells (Figure 2D). Noteworthy, other EGFR ligands like EGF, amphiregulin and heparin-binding EGF were not affected by hypoxia (data not shown). We also found that TGF-α messenger RNA levels were upregulated by hypoxic stress in control siRNA HN6 cells, but returned to normoxic, basal levels in cells where HIF-2α was knocked down (Figure 2E). Our results also revealed major differences between HN4 cells, which lack the hypoxic EGFR activation response, and HN6 cells. In this regard, EGFR expression levels were markedly increased in HN6 cells regardless of oxygen concentration; however, TGF-α levels were upregulated only in hypoxic HN6 cells (Figure 2F). Overall, these findings pointed to HIF-2α as the main HIF-α promoting upstream molecular events to trigger the hypoxic activation of the EGFR pathway in HNSCC cells. In addition, our data suggested that TGF-α might be a key intervening ligand triggering hypoxic EGFR activation in highly expressing EGFR HNSCC cells.

Hypoxia induces a motile phenotype in HNSCC cells

To investigate the biological significance underlying hypoxic EGFR activation in HNSCC cells, we first examined whether exposure to hypoxia led to a proliferative advantage in moderately versus highly EGFR-expressing cells. After exposing HN4 and HN6 cells to low oxygen concentrations for 72 h, we found no increase in cell proliferation in any of the cell lines (Figure 3A). These results implied that hypoxic EGFR activation was not triggering a mitogenic response but possibly mediating other oncogenic processes. To this end, strong

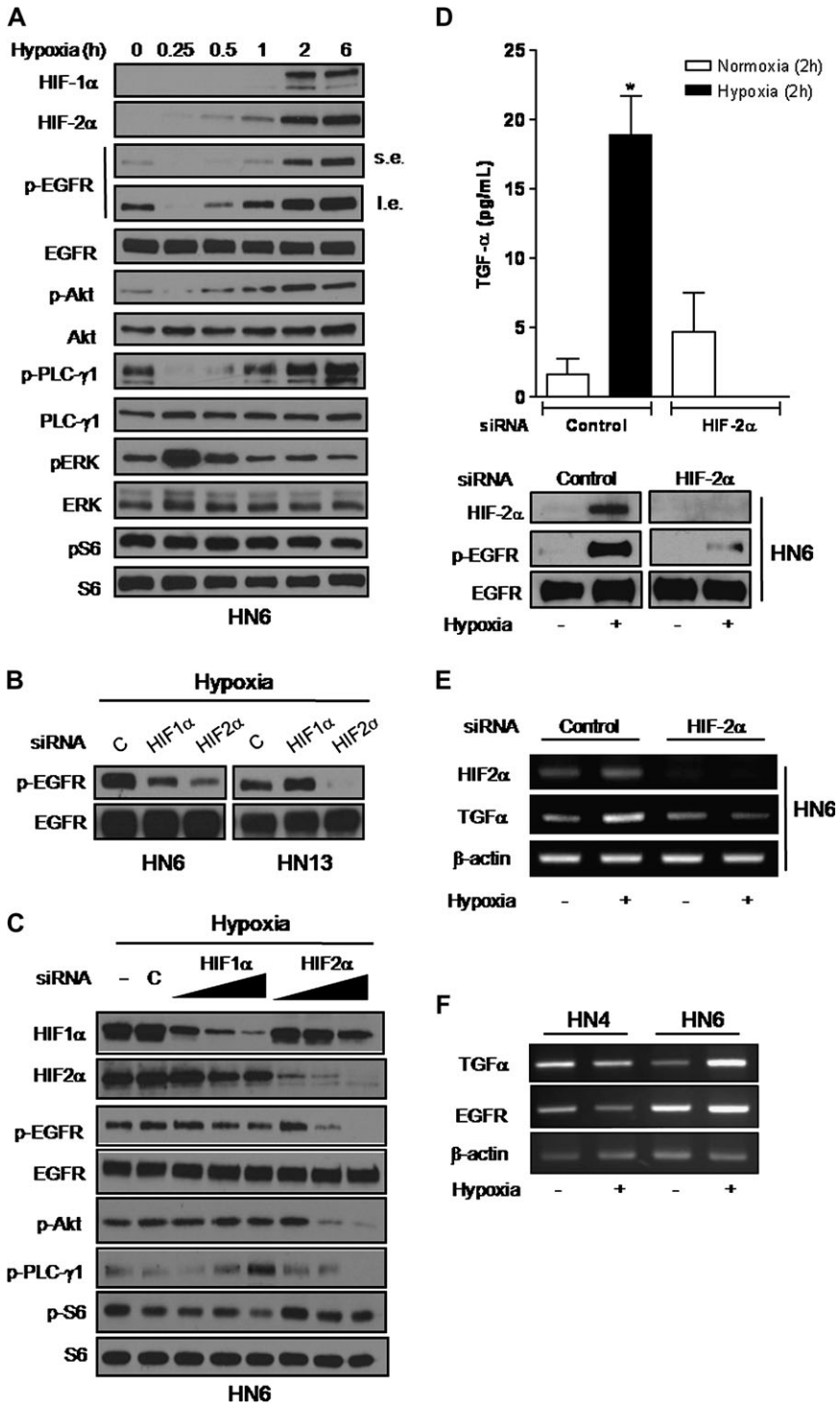

Fig. 2. HIF-2α mediates hypoxic EGFR signaling activation. (**A**) HN6 cells exposed to hypoxia for the indicated times were analyzed by western blotting with primary antibodies against HIF-1α, HIF-2α and proteins related to the EGFR signaling pathway. Signals for phosphorylated EGFR (pEGFR) expression were obtained after short (s.e.) and long (l.e.) radiographic exposure. (**B**) Serum-starved HN6 and HN13 cells transfected with 10 nM of either non-targeted control (**c**), HIF-1α or HIF-2α siRNA were exposed to hypoxia for 6 h. Western blot analyses showed expression levels of total and phosphorylated EGFR. (**C**), whole cell lysates from serum-deprived parental HN6 cells (−), HN6 cells transfected with non-targeted control siRNA (c; 20 nM) or increasing doses of HIF-1α or HIF-2α siRNAs (5–20 nM) were obtained following 6 h of hypoxia and utilized for immunoblotting to assess phosphorylated status of EGFR, Akt, PLC-γ1 and S6. (**D**) TGF-α levels in conditioned medium from control siRNA or HIF-2α–siRNA-transfected HN6 cells cultured under normoxic or hypoxic conditions for 2 h were determined by enzyme-linked immunosorbent assay (top panel), $^{*}P < 0.01$ versus normoxic control siRNA, HIF-2α siRNA as well as hypoxic HIF-2α siRNA cells. Western blotting confirmed HIF-2α knocked down and lack of EGFR phosphorylation in hypoxic HIF-2α siRNA-transfected cells (bottom panel). (**E**) Total RNA was isolated from HN6 cells transfected with either control siRNA or HIF-2α siRNA cultured under normoxic or hypoxic conditions for 2 h. Following reverse transcription of 2 μg total RNA, HIF-2α and TGF-α messenger RNA levels were detected by PCR. β-actin was used as an internal control for equal loading. (**F**) Total RNA was isolated from HN4 and HN6 cells cultured under normoxia or hypoxia for 6 h. Following reverse transcription of 2 μg total RNA, HIF–TGF-α and EGFR messenger RNA levels were detected by PCR. β-Actin was used as an internal control for equal loading.

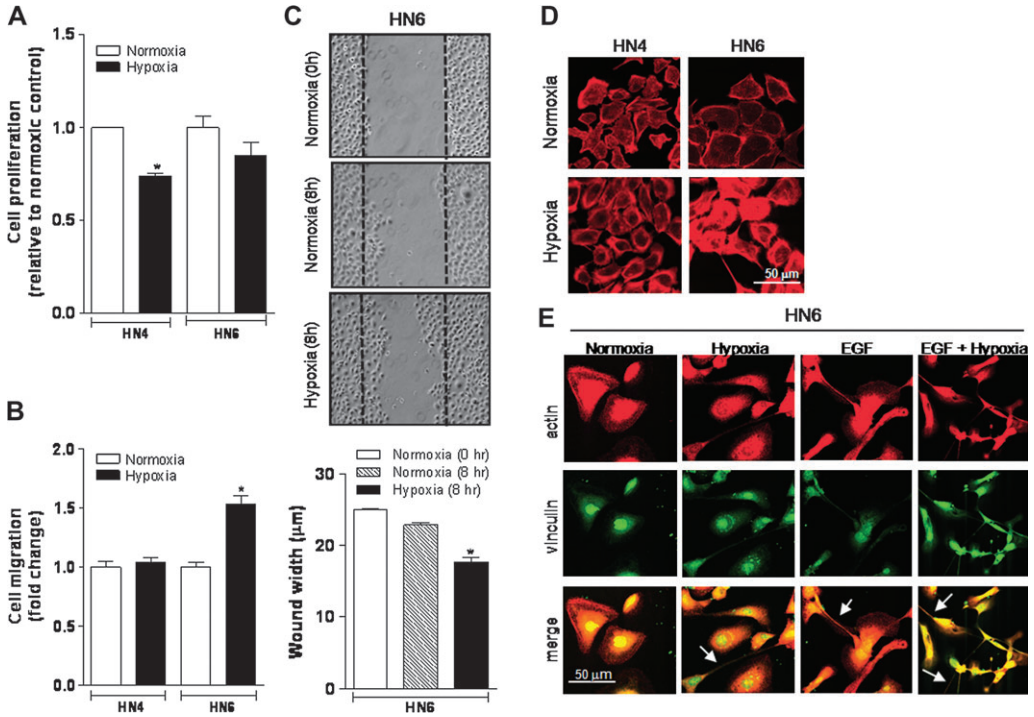

Fig. 3. Hypoxia enhances HNSCC cell motility and triggers changes in cell shape. (**A**) HN4 and HN6 cell proliferation was determined by the MTS assay following 72 h of incubation in either normoxia or hypoxia. Data are presented as fold change relative to normoxic controls. $^{*}P < 0.05$ versus normoxic HN4 cells. (**B**) Migration of serum-starved HN4 and HN6 cells was evaluated through an *in vitro* colorimetric assay. After a 5-h exposure to either normoxia or hypoxia, cells migrating through a polycarbonate filter were stained and the optical density of the extracted dye was detected on a microplate reader at 560 nm. Data are presented as fold change relative to the normoxic control of each HNSCC cell line. $^{*}P < 0.0001$ versus normoxic controls. (**C**) Wound closure motility assay was also performed in serum-starved HN6 cells exposed to normoxia or hypoxia for 8 h. Ten regions of the remaining acellular area between wound margins were randomly selected to calculate the average wound width per scratch in micrometers. $^{*}P < 0.0001$ versus normoxic controls. (**D**) Rhodamine–phalloidin staining shows marked redistribution of the actin cytoskeleton only in HN6 cells compared with HN4 cells following 6 h of hypoxia. (**E**) Confocal microscopy image of serum-starved HN6 cells exposed for 8 h to normoxia or hypoxia in the presence or absence of EGF (100 ng/ml) and immunostained with antibodies to actin (red) and vinculin (green). Marked changes in cell shape with the formation of protrusive membrane structures (arrows) are clearly identified following exposure to hypoxia and/or EGF.

evidence supports a major influence of the EGFR signaling pathway on tumor cell invasion and migration in head and neck cancer, especially when coupled to PLC-γ1 activation (30,31). Therefore, we explored whether hypoxia had any impact on HNSCC cell migratory capacity. Through a modified Boyden chamber migration assay carried out to assess variations in the migratory competency of hypoxic HN4 and HN6 cells, we found that reduced oxygenation elicited a significant increase in HN6 cell migration (1.5-fold increase versus normoxic controls). Conversely, hypoxic exposure resulted in no difference in HN4 cell motility (Figure 3B). These findings were supported by results obtained using an *in vitro* wound closure motility assay as previously described (27). We found that an increased number of hypoxic HN6 cells migrated toward an acellular area, suggesting an enhanced motile potential (Figure 3C). These findings revealed that in a subset of HNSCC cells, reduced oxygenating conditions may act as a potent stimulus to promote cell motility by inducing the activation of the EGFR signaling pathway.

Hypoxia promotes changes in HNSCC cell shape and actin redistribution

To evaluate whether oxygen levels had any impact on the distribution of the actin cytoskeleton, we stained HN4 and HN6 cells with rhodamine–phalloidin following their incubation under normoxia or hypoxia for 8 h. A significant change in the distribution of the actin cytoskeleton was observed only in hypoxic HN6 cells as compared with their normoxic controls or HN4 cells grown under similar conditions. Hypoxic HN6 cells showed typical features of actin cytoskeletal cellular redistribution (Figure 3D). Consistent with these findings, an unexpected change in cell shape characterized by the formation of rod-like protrusions resembling actin-based filopodia (32) were observed in hypoxic HN6 cells in the presence or absence of exogenous EGF (Figure 3E). These changes were evident after immunostaining cells with antibodies against key cytoskeletal proteins such as actin and vinculin following previously published methods (27). Whereas normoxic HN6 cells appeared polygonal and spread, the sole exposure to either hypoxia or EGF induced morphological changes consistent with a more spindle-shaped, fibroblastic-like morphology. These morphological changes appeared more accentuated when hypoxic HN6 cells were cultured in the presence of EGF.

EGFR/PLC-γ1 activation promotes actin cytoskeletal reorganization and enhances cell migration in hypoxic HNSCC cells

The acquisition of a motile phenotype is a key step in the progression to metastasis in a variety of epithelial tumors. Thus, a better understanding of the molecular events controlling cell migration is critically needed, especially in HNSCC, where locoregional invasion and nodal involvement are often associated with impaired patient prognosis (6). The main mechanism affecting the development of the motile phenotype in cancer cells involves the reorganization of the actin cytoskeleton (33). Because of the striking inhibition of the EGFR/PLC-γ1 pathway in hypoxic HIF-2α siRNA-transfected HN6 cells, we next examined whether inhibition of either EGFR tyrosine kinase or PLC activities were capable of altering hypoxic HN6 cell motility and actin distribution. Whereas cell migration was significantly increased in hypoxic cells, the presence of the inhibitors markedly reduced their migratory capacity (Figure 4A). These findings were supported by immunoblotting results showing a significant reduction in the phosphorylated status of EGFR, Akt and PLC-γ1 when hypoxic HN6 cells were

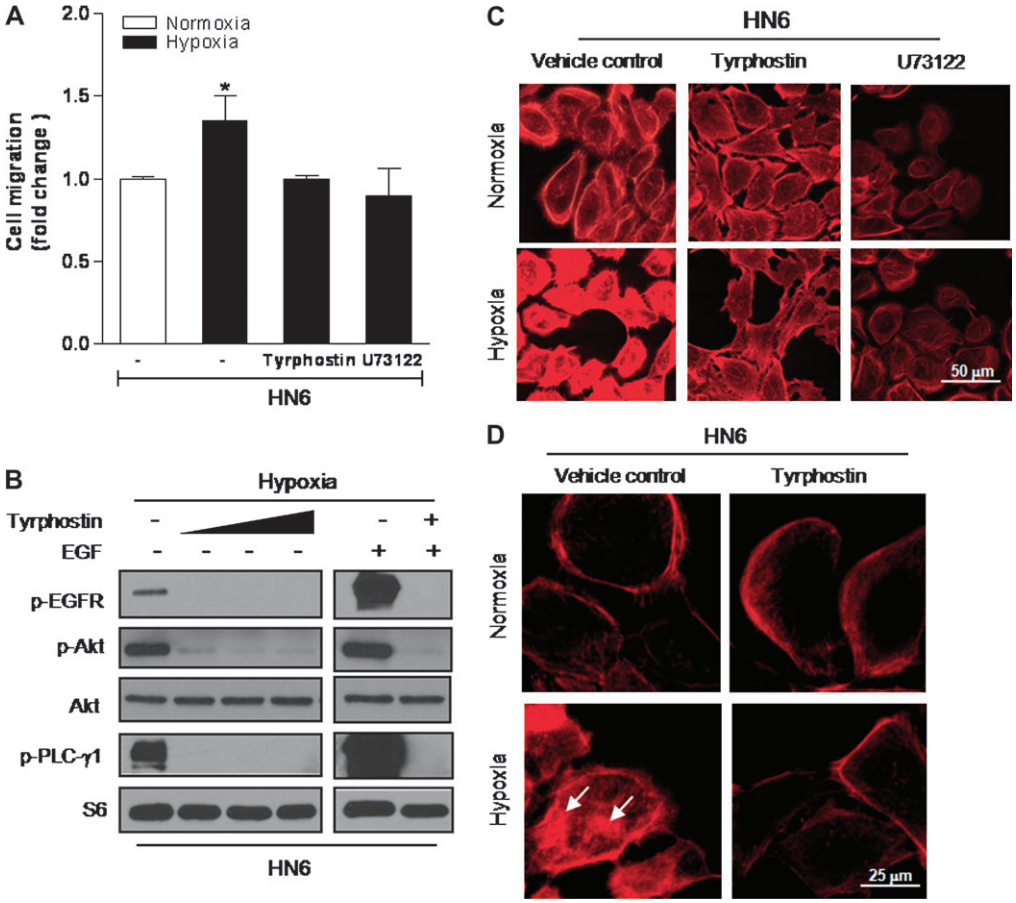

Fig. 4. Inhibition of EGFR/PLC-γ1 activation blocks actin redistribution and cell migration. (**A**) Pretreatment with the EGFR tyrosine kinase inhibitor tyrphostin (25 μM) or U73122 (3 μM) inhibited the increased migratory capacity of hypoxic cells. (**B**) HN6 cells were exposed to hypoxia for 6 h in the presence or absence of increasing concentrations of tyrphostin (5–50 μM). Western blotting evaluated phosphorylated status of EGFR, Akt and PLC-γ1. EGF (100 ng/ml) was used as a positive control for EGFR-mediated signaling. S6 was used as sample loading control. (**C**) Actin cytoskeletal changes were prevented following pretreatment with tyrphostin (25 μM) or U73122 (3 μM) prior to 6-h exposure to hypoxia. (**D**) Higher magnification image depicts redistribution of actin aggregates in hypoxic cells (arrows) when compared with normoxic controls or cells pretreated with tyrphostin (25 μM).

cultured in the presence of tyrphostin (Figure 4B). These data provided more evidence on the major role that hypoxia played in enhancing the motility of highly EGFR-expressing cells. Furthermore, actin cytoskeletal redistribution, as judged by the presence of increased actin aggregates, was clearly affected when hypoxic HN6 cells were incubated with tyrphostin or U73122 (Figure 4C and D), highlighting a key role of the EGFR/PLC-γ1 signaling axis in mediating the development of a motile phenotype in response to hypoxia.

Targeting HIF-2α blocks migratory capacity of hypoxic HNSCC cells

Because our results indicated a close association between HIF-2α with the activation of EGFR and downstream signaling factors in hypoxic HNSCC cells, we next evaluated whether selective targeting of HIF-2α by RNA interference prevented changes in actin redistribution observed in hypoxic HN6 cells. Noticeably, our data demonstrated that actin reorganization induced by hypoxia in control siRNA-transfected HN6 cells was markedly reduced by knocking down HIF-2α (Figure 5A). Indeed, HN6 control siRNA-transfected cells exposed to hypoxia showed increased motility when compared with hypoxic HIF-2α siRNA-transfected cells (Figure 5B). Emerging evidence points to the inhibition of the HIF system as a viable approach to control cancer progression. Through this strategy, downregulation of many HIF-controlled genes and their encoded proteins that are critical for tumor cell survival, angiogenesis and metastasis can be achieved (34,35). In this regard, cancer chemotherapeutics agents like topotecan and etoposide, which act as inhibitors of topoisomerase I and II, respectively, have revealed promising *in vitro* and preclinical results in controlling HIF-1 accumulation and activity, independently of their cytotoxic effects (36,37). To investigate whether HIF-2α-mediated EGFR activation could be blocked by etoposide, hypoxic HN6 cells were cultured in the presence of increasing doses of this agent for 2 h. We observed that in etoposide-treated hypoxic cells, HIF-2α and the phosphorylated levels of EGFR were significantly decreased in a dose-dependent manner, without affecting total EGFR expression levels (Figure 5C). As seen in Figure 5D, etoposide treatment also led to a decrease in the migratory response of hypoxic cells comparable with the reduction observed with the EGFR tyrosine kinase or PLC inhibitors (Figure 5A). Overall, these results validate the key role that HIF-2α is playing on the control of the EGFR pathway in a subset of HNSCC cells. Furthermore, we show that under hypoxic conditions, the topoisomerase inhibitor etoposide is able to block HIF-2α accumulation, prevent EGFR activation and disrupt HNSCC cell migration.

EGFR is phosphorylated within hypoxic foci in human HNSCC tumors

To confirm whether our *in vitro* findings provide translational clinical relevance, we next evaluated the phosphorylation status of EGFR by immunohistochemistry within areas of hypoxia in human-derived HNSCC tumors as judged by the pattern of regional distribution of HIF-2α immunostaining. Whereas EGFR levels were markedly upregulated in all the tumor samples examined ($n = 11$), variable phosphorylated EGFR staining occurred in a fraction of invasive,

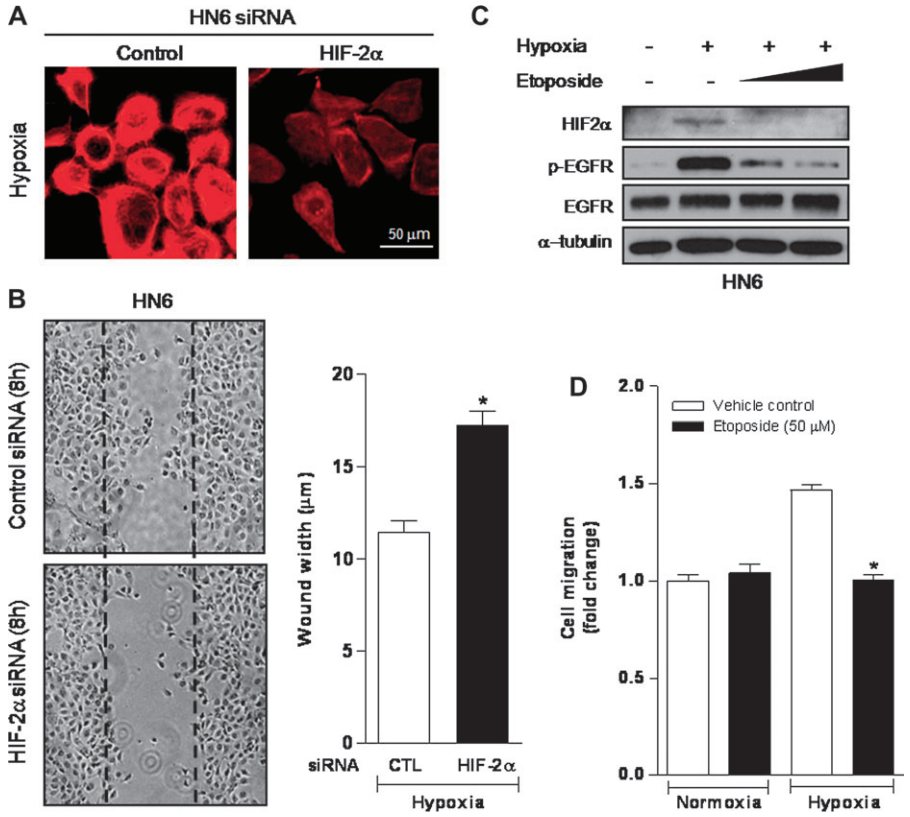

Fig. 5. Targeting HIF-2α negatively impacts hypoxic EGFR activation and cell migration. (**A**) HIF-2α siRNA prevents actin cytoskeletal changes in hypoxic HN6 cells. (**B**) Wound closure motility assay shows reduced capacity of HIF-2α siRNA-transfected HN6 cells to migrate after exposure to hypoxia for 8 h. $^{*}P < 0.001$. (**C**) Dose-dependent inhibition of hypoxia-induced activation of HIF-2α and EGFR by etoposide (25–50 μM) in HN6 cells exposed to hypoxia for 2 h. (**D**) Treatment with etoposide inhibited the increased migratory capacity triggered by a 6-h hypoxic exposure in HN6 cells. $^{*}P < 0.001$.

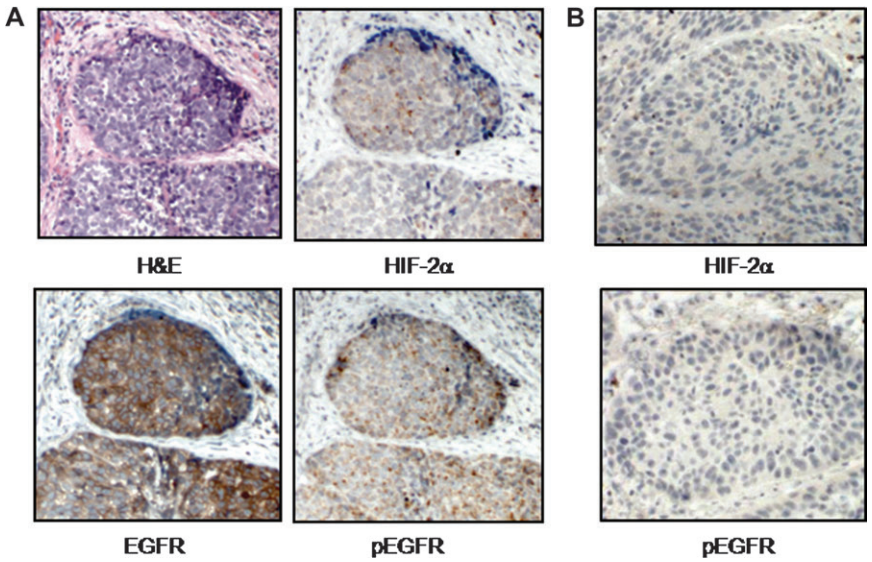

Fig. 6. EGFR phosphorylation within hypoxic tumor foci in human HNSCC. (**A**) Representative human HNSCC specimen where immunohistochemistry was performed using antibodies against HIF-2α, total EGFR and phospho-EGFR along with hematoxylin and eosin (H&E). Phospho-EGFR staining was detected within hypoxic areas as judged by HIF-2α accumulation. (**B**) Another representative HNSCC specimen in which HIF-2α immunostaining was negative, undetectable levels of phospho-EGFR were found. Magnification, ×100.

moderately to poorly differentiated tumors (8 of the 11 tumors evaluated; 72.7%; Figure 6A and B). Of note, whereas the expression levels of phospho-EGFR and HIF-2α spatially fluctuated within a single tumor possibly because of the heterogeneous nature of intratumoral oxygenation, we consistently observed phosphorylated forms of EGFR in the vicinity of HIF-2α expression within hypoxic foci. Overall, our findings position HIF-2α as a novel regulator of EGFR activation under hypoxic conditions, and suggest that hypoxia-induced EGFR signaling may promote a more aggressive phenotype in a subset of HNSCC tumors.

Discussion

Multiple studies agree that the altered expression of EGFR is a critical determinant of tumor progression in a variety of solid tumors (20,38). In head and neck cancer, increased *EGFR* copy number and overexpression of EGFR and its ligands are considered strong negative predictors of patient survival (22,23). Activation of molecular pathways downstream of the EGFR often results in the promotion of oncogenic activities leading to tumor cell growth, cell survival and metastasis (29,39). As a consequence, targeted therapies to inhibit EGFR activity complemented by standard chemoradiation have become common components of clinical protocols designed to deter disease progression (21). In spite of the significant progress achieved in developing therapeutic strategies to selectively inhibit EGFR activity, only modest results have been obtained in the clinic (40). Elucidating novel mechanisms underlying EGFR activation in HNSCC may unravel new information to help improving overall clinical outcomes. The work presented here was aimed at gaining insight into the role of hypoxic stress on EGFR activity in HNSCC.

Poorly oxygenated areas resulting in part from a structurally and functionally aberrant vasculature are commonly found within heterogeneous regions of expanding HNSCC tumors (7,8). The presence of intratumoral hypoxia relative to the expression of HIF-1α and HIF-2α has been consistently regarded as a major negative factor in head and neck cancer, especially when it relates to locoregional disease control and patient survival following radiation therapy (10,41). Although intratumoral hypoxia and the EGFR pathway independently promote HNSCC oncogenesis, the potential effects of low oxygenation on EGFR activity in this cancer type has received little attention. To this end, we hypothesized that the presence of an intratumoral hypoxic microenvironment may serve as a potent stimulus to increase cancer aggressiveness by controlling cues directed at activating the EGFR signaling pathway. We show that moderate hypoxia, represented experimentally by the exposure to 1% O_2, leads to a selective HIF-2α-mediated EGFR pathway activation only in HNSCC cells highly overexpressing EGFR levels. Furthermore, our immunohistochemical data demonstrate that in a fraction of aggressive human HNSCC tumors, EGFR phosphorylation occurs within areas of low oxygenation as evidenced by HIF-2α immunostaining.

Our findings point to hypoxia-induced TGF-α as a potential trigger for EGFR activation in this subset of HNSCC cells; nevertheless, we do not rule out the possibility that other growth factors or cytokines may also be participating in the induction of EGFR activation. There is strong evidence demonstrating that HIF-2α is the main transcriptional activator of TGF-α in cell lines derived from VHL-defective clear cell renal cell carcinoma, the most frequent kidney malignancy in humans (15). In VHL-defective renal cell carcinoma cells, HIFα polyubiquitination and proteasomal degradation are blocked in an oxygen concentration-independent manner leading to HIF-1 and HIF-2 stabilization and activity. Of note, TGF-α is known as the only mitogenic EGFR ligand with VHL-dependent expression profiles, and HIF2α inhibition is sufficient to suppress VHL-defective tumor growth by affecting the TGF-α/EGFR signaling axis (15,42). These responses highlight the notion that although HIF-1α and HIF- 2α are structurally similar in their DNA binding and dimerization domains, variations in their transactivation domains provide non-overlapping characteristics to differentially regulate hypoxic responsive genes (43). In fact, HIF-2α controls a number of hypoxia-inducible genes, which encode proteins closely associated with more aggressive tumor phenotypes. Among these are proteins promoting tumor cell proliferation (i.e., cyclin D1; c-myc), angiogenesis (i.e., vascular endothelial growth factor, erythropoietin. angiopoietin) and epithelial to mesenchymal transition/metastasis (i.e., E-cadherin. CXCR4, lysil oxidase, TWIST) (44). In our study, striking morphological changes represented by the marked redistribution of the actin cytoskeleton and the formation of filopodia-like protrusions accompanied an enhanced migratory capacity. These morphological and motile responses were effectively prevented when inhibitors of the EGFR pathway including the tyrosine kinase inhibitor tyrphostin and the PLC inhibitor U73122 were used prior to hypoxic exposure. These results are in agreement with previous studies demonstrating the critical role of the EGFR/PLC-γ1 pathway in promoting HNSCC cell motility and invasion in response to EGFR ligand stimulation under atmospheric conditions (31). Furthermore, the role of HIF-2α in enhancing the migratory competency of EGFR-overexpressing HNSCC cells was also validated by suppressing HIF-2α accumulation through siRNA techniques or pharmacologically by using the topoisomerase II inhibitor etoposide. As emerging studies demonstrate in other cancer cell types, the use of topoisomerase poisons such as topotecan and etoposide in doses that are unrelated to their cytotoxic effects may prove to be beneficial in preventing HIFα accumulation (36,37,45). As a matter of fact, novel therapeutic approaches are being proposed to more effectively control the hypoxic response and tumor angiogenesis through the combination of vascular endothelial growth factor-targeted therapies with topoisomerase inhibitors (46).

Considering the major role EGFR and TGF-α expression levels play in HNSCC progression (22–24), our study provides the first indication that HIF-2α may also be a critical factor promoting tumor aggressiveness in response to hypoxia by mediating the activation of the EGFR pathway in a subset of HNSCC patients. Further studies are warranted to characterize the expression and secretion patterns of TGF-α, in particular, and other growth factors and cytokines relative to the hypoxic response in highly EGFR-expressing cell lines as well as in human HNSCC. It is plausible that in a fraction of hypoxic HNSCC tumors, EGFR overexpression in concert with the selective production of hypoxia-induced EGFR cognate ligands or possibly other EGFR transactivating factors orchestrate an autocrine, paracrine and/or juxtacrine stimulus to further sustain a more aggressive tumor behavior. Because hypoxic tumors are commonly resistant to chemotherapy, it is probable that the persistent hypoxic activation of the EGFR pathway may negatively impact the sensitivity to EGFR-targeted therapies in a subset of head and neck cancer patients bearing hypoxic tumors. To this end, combination therapies that target both the hypoxic response and the EGFR pathway may become an attractive strategy to control HNSCC development and progression.

Funding

National Institutes of Health Training Program in Oral and Craniofacial Biology (5T32DE007309-11 to A.S.); University of Maryland Greenebaum Cancer Center-American Cancer Society Institutional Research (IRG-97-153-07, pilot grant to A.S.); University of Maryland Dental School (to A.S.).

Acknowledgements

We thank Drs Meenakshi Chellaiah and John Basile (Oncology and Diagnostic Sciences) for assistance with confocal microscopy and histopathology, respectively. We also thank Dr Li Mao (Oncology and Diagnostic Sciences) for helpful discussions.

Conflict of Interest Statement: None declared.

References

1. Hanahan,D. *et al*. (2000) The hallmarks of cancer. *Cell*, **100**, 57–70.
2. Gatenby,R.A. *et al*. (2004) Why do cancers have high aerobic glycolysis? *Nat. Rev. Cancer*, **4**, 891–899.
3. DeBerardinis,R.J. *et al*. (2008) The biology of cancer: metabolic reprogramming fuels cell growth and proliferation. *Cell Metab.*, **7**, 11–20.
4. Jemal,A. *et al*. (2009) Cancer statistics, 2009. *CA Cancer J. Clin.*, **59**, 225–249.
5. Seiwert,T.Y. *et al*. (2007) The chemoradiation paradigm in head and neck cancer. *Nat. Clin. Pract. Oncol.*, **4**, 156–171.
6. Kelley,L.C. *et al*. (2008) Actin cytoskeletal mediators of motility and invasion amplified and overexpressed in head and neck cancer. *Clin. Exp. Metastasis*, **25**, 289–304.
7. Isa,A.Y. *et al*. (2006) Hypoxia in head and neck cancer. *Br. J. Radiol.*, **79**, 791–798.

8. Janssen,H.L. *et al*. (2005) Hypoxia in head and neck cancer: how much, how important? *Head Neck*, **27**, 622–638.
9. Bacon,A.L. *et al*. (2004) Hypoxia-inducible factors and hypoxic cell death in tumour physiology. *Ann. Med.*, **36**, 530–539.
10. Aebersold,D.M. *et al*. (2001) Expression of hypoxia-inducible factor-1 alpha: a novel predictive and prognostic parameter in the radiotherapy of oropharyngeal cancer. *Cancer Res.*, **61**, 2911–2916.
11. Semenza,G.L. (2009) Regulation of cancer cell metabolism by hypoxia-inducible factor 1. *Semin. Cancer Biol.*, **19**, 12–16.
12. Kaelin,W.G.Jr. (2008) The von Hippel-Lindau tumour suppressor protein: O2 sensing and cancer. *Nat. Rev. Cancer*, **8**, 865–873.
13. Mahon,P.C. *et al*. (2001) FIH-1: a novel protein that interacts with HIF-1alpha and VHL to mediate repression of HIF-1 transcriptional activity. *Genes Dev.*, **15**, 2675–2686.
14. Lando,D. *et al*. (2002) FIH-1 is an asparaginyl hydroxylase enzyme that regulates the transcriptional activity of hypoxia-inducible factor. *Genes Dev.*, **16**, 1466–1471.
15. Gunaratnam,L. *et al*. (2003) Hypoxia inducible factor activates the transforming growth factor-alpha/epidermal growth factor receptor growth stimulatory pathway in VHL(-/-) renal cell carcinoma cells. *J. Biol. Chem.*, **278**, 44966–44974.
16. Smith,K. *et al*. (2005) Silencing of epidermal growth factor receptor suppresses hypoxia-inducible factor-2-driven VHL-/- renal cancer. *Cancer Res.*, **65**, 5221–5230.
17. Franovic,A. *et al*. (2007) Translational up-regulation of the EGFR by tumor hypoxia provides a nonmutational explanation for its overexpression in human cancer. *Proc. Natl Acad. Sci. U S A.*, **104**, 13092–13097.
18. Wang,Y. *et al*. (2009) Regulation of endocytosis via the oxygen-sensing pathway. *Nat. Med.*, **15**, 319–324.
19. Franovic,A. *et al*. (2009) Human cancers converge at the HIF-2alpha oncogenic axis. *Proc. Natl Acad. Sci. U S A.*, **106**, 21306–21311.
20. Hynes,N.E. *et al*. (2009) ErbB receptors and signaling pathways in cancer. *Curr. Opin. Cell Biol.*, **21**, 177–184.
21. Harari,P.M. *et al*. (2009) Molecular target approaches in head and neck cancer: epidermal growth factor receptor and beyond. *Semin. Radiat. Oncol.*, **19**, 63–68.
22. Rubin Grandis,J. *et al*. (1998) Levels of TGF-alpha and EGFR protein in head and neck squamous cell carcinoma and patient survival. *J. Natl Cancer Inst.*, **90**, 824–832.
23. Temam,S. *et al*. (2007) Epidermal growth factor receptor copy number alterations correlate with poor clinical outcome in patients with head and neck squamous cancer. *J. Clin. Oncol.*, **25**, 2164–2170.
24. Kumar,B. *et al*. (2008) EGFR, p16, HPV Titer, Bcl-xL and p53, sex, and smoking as indicators of response to therapy and survival in oropharyngeal cancer. *J. Clin. Oncol.*, **26**, 3128–3137.
25. Jeon,G.A. *et al*. (2004) Global gene expression profiles of human head and neck squamous carcinoma cell lines. *Int. J. Cancer*, **112**, 249–258.
26. Schneider,A. *et al*. (2008) Hypoxia-induced energy stress inhibits the mTOR pathway by activating an AMPK/REDD1 signaling axis in head and neck squamous cell carcinoma. *Neoplasia*, **10**, 1295–1302.
27. Samanna,V. *et al*. (2006) Alpha-V-dependent outside-in signaling is required for the regulation of CD44 surface expression, MMP-2 secretion, and cell migration by osteopontin in human melanoma cells. *Exp. Cell Res.*, **312**, 2214–2230.
28. Sriuranpong,V. *et al*. (2003) Epidermal growth factor receptor-independent constitutive activation of STAT3 in head and neck squamous cell carcinoma is mediated by the autocrine/paracrine stimulation of the interleukin 6/gp130 cytokine system. *Cancer Res.*, **63**, 2948–2956.
29. Morgan,S. *et al*. (2009) ErbB receptors in the biology and pathology of the aerodigestive tract. *Exp. Cell Res.*, **315**, 572–582.
30. Wells,A. *et al*. (2003) Phospholipase C-gamma1 in tumor progression. *Clin. Exp. Metastasis*, **20**, 285–290.
31. Thomas,S.M. *et al*. (2003) Epidermal growth factor receptor-stimulated activation of phospholipase Cgamma-1 promotes invasion of head and neck squamous cell carcinoma. *Cancer Res.*, **63**, 5629–5635.
32. Gupton,S.L. *et al*. (2007) Filopodia: the fingers that do the walking. *Sci. STKE*, **400**, re5. 1–8.
33. Yamazaki,D. *et al*. (2005) Regulation of cancer cell motility through actin reorganization. *Cancer Sci.*, **96**, 379–386.
34. Semenza,G.L. (2007) Evaluation of HIF-1 inhibitors as anticancer agents. *Drug Discov. Today*, **12**, 853–859.
35. Onnis,B. *et al*. (2009) Development of HIF-1 inhibitors for cancer therapy. *J. Cell. Mol. Med.*, **13**, 2780–2786.
36. Rapisarda,A. *et al*. (2004) Topoisomerase I-mediated inhibition of hypoxia-inducible factor 1: mechanism and therapeutic implications. *Cancer Res.*, **64**, 1475–1482.
37. Choi,Y.J. *et al*. (2009) HIF-1alpha modulation by topoisomerase inhibitors in non-small cell lung cancer cell lines. *J. Cancer Res. Clin. Oncol.*, **135**, 1047–1053.
38. Baselga,J. *et al*. (2005) Critical update and emerging trends in epidermal growth factor receptor targeting in cancer. *J. Clin. Oncol.*, **23**, 2445–2459.
39. Rogers,S.J. *et al*. (2005) Biological significance of c-erbB family oncogenes in head and neck cancer. *Cancer Metastasis Rev.*, **24**, 47–69.
40. Dutta,P.R. *et al*. (2007) Cellular responses to EGFR inhibitors and their relevance to cancer therapy. *Cancer Lett.*, **254**, 165–177.
41. Koukourakis,M.I. *et al*. (2006) Endogenous markers of two separate hypoxia response pathways (hypoxia inducible factor 2 alpha and carbonic anhydrase 9) are associated with radiotherapy failure in head and neck cancer patients recruited in the CHART randomized trial. *J. Clin. Oncol.*, **24**, 727–735.
42. Kondo,K. *et al*. (2003) Inhibition of HIF2alpha is sufficient to suppress pVHL-defective tumor growth. *PLoS Biol.*, **1**, E83.
43. Hu,C.J. *et al*. (2003) Differential roles of hypoxia-inducible factor 1alpha (HIF-1alpha) and HIF-2alpha in hypoxic gene regulation. *Mol. Cell. Biol.*, **23**, 9361–9374.
44. Qing,G. *et al*. (2009) Hypoxia inducible factor-2alpha: a critical mediator of aggressive tumor phenotypes. *Curr. Opin. Genet. Dev.*, **19**, 60–66.
45. Rapisarda,A. *et al*. (2004) Schedule-dependent inhibition of hypoxia-inducible factor-1alpha protein accumulation, angiogenesis, and tumor growth by topotecan in U251-HRE glioblastoma xenografts. *Cancer Res.*, **64**, 6845–6848.
46. Rapisarda,A. *et al*. (2009) Increased antitumor activity of bevacizumab in combination with hypoxia inducible factor-1 inhibition. *Mol. Cancer Ther.*, **8**, 1867–1877.

Received November 12, 2009; revised March 19, 2010; accepted April 10, 2010